

PAPER • OPEN ACCESS

## Features of Shear Banding in Grains with Orientation $\{111\}<110>$ in the Fe – 3%Si Alloy

To cite this article: M L Lobanov *et al* 2020 *IOP Conf. Ser.: Mater. Sci. Eng.* **969** 012032

View the [article online](#) for updates and enhancements.



The Electrochemical Society  
Advancing solid state & electrochemical science & technology  
2021 Virtual Education

**Fundamentals of Electrochemistry:**  
Basic Theory and Kinetic Methods  
Instructed by: **Dr. James Noël**  
Sun, Sept 19 & Mon, Sept 20 at 12h–15h ET

Register early and save!



## Features of Shear Banding in Grains with Orientation $\{111\}\langle 110 \rangle$ in the Fe–3%Si Alloy

M L Lobanov<sup>1,2</sup>, P L Reznik<sup>1</sup> and A A Redikultsev<sup>1</sup>

<sup>1</sup>Ural Federal University named after the first President of Russia B. N. Yeltsin, 19, Mira st., Ekaterinburg, 620002, Russia

<sup>2</sup>M. N. Mikheev Institute of Metal Physics of Ural Branch of the Russian Academy of Sciences, 18, S. Kovalevskaya st., Ekaterinburg, 620990, Russia

E-mail: m.l.lobanov@urfu.ru

**Abstract.** EBSD method were used to study the texture of BCC crystals  $\{111\}\langle 110 \rangle$  Fe-3%Si. It is shown that in the state after cold rolling shear bands with habit plane at a slope of  $\sim 20\text{--}40^\circ$  to the RD were formed as a result of 70% deformation. Theoretical analysis was performed and experimental data were analyzed which showed that the matrix reorientation into orientation  $\{110\}\langle 001 \rangle$  occurs when grain stripping with orientation  $\{111\}\langle 110 \rangle$ . Such effects are observed either due to rotation around the  $\langle 100 \rangle$  axis or due to rotation around the  $\langle 110 \rangle$  axis. By means of dislocation sliding, most of the SBs blocks are reoriented to orientations close to  $\{111\}\langle 112 \rangle$ .

### 1. Introduction

Transformations, which determine the structure and texture of grain electrotechnical steel or Fe – 3% Si alloy (GOES) are caused by formation of sharp texture  $\{110\}\langle 001 \rangle$  at one of the final stages of steel processing [1, 2], are not fully understood. One of the most important tasks in the process of texture formation in GOES is to create orientation  $\{110\}\langle 001 \rangle$ . This can be achieved due to operations preceding secondary recrystallization. After significant cold deformation, the areas of orientation  $\{110\}\langle 001 \rangle$  are formed in shear bands (SBs). Shift bands appear in crystallites  $\{111\}\langle 112 \rangle$ , such areas then develop at primary recrystallization [3–7].

From the research point of view, the most mysterious element of the deformation mesostructure is SB. To date, a large amount of experimental data [8–17] on their morphology, the correlation between the matrix and crystallite orientation in the stripes, and their location in the matrix have been accumulated. Theoretical views of their formation are presented in detail in [18–23]. However, not all aspects of this issue are considered in them.

The main prerequisite for the formation of shear bands in crystals, i.e., loss of stability of homogeneous deformation, is the “hardness” of its orientation, characterized by a large Taylor coefficient [14]. The Dillmore theory assumes that strong localization of deformation in SB promotes macroscopic deformation of a crystal even without changing its orientation as a whole [18]. When rolling metal, regardless of the type of its crystal lattice, the SB should be located at angles close to  $\pm 35^\circ$  to the rolling plane. Formation of SB has another important aspect that connects the reorientation of the crystal lattice inside them with the geometric softening inside the plasticity model of Taylor [24]. SBs are treated as areas where the shift deformation is localized. However, little is known about their



internal structure and formation during cold rolling. Thus, it is important to study the basic laws of shear band formation to understand texture formation in GOES.

However, little is known about the internal structure of SPs when they are formed during cold rolling. Hence, it is necessary to study the basic laws of shear band formation. This approach can be useful for understanding texture formation in GOES.

Observation of texture evolution during secondary recrystallization shows that orientation  $\{111\}\langle 112 \rangle$  is the main one, which is "absorbed" in the first place. This process is also related to SBs crystallography. Establishing this connection is also an important part of the problem to be solved. Orientation  $\{111\}\langle 112 \rangle$  is dominant in the surface layers - the result of primary recrystallization GOES. It is likely that in the dominant after deformation orientations  $\{111\}\langle 110 \rangle$ ,  $\{112\}\langle 110 \rangle$  SBs are the main "candidate" for the sources of grain formation with the orientation  $\{111\}\langle 112 \rangle$ .

Presentation of results of research of Fe-3% Si alloy in the state of cold deformation, in which shear bands were formed in grains with orientation  $\{111\}\langle 110 \rangle$  is the purpose of this paper.

## 2. Materials and methods

Samples were taken from a 0.65 mm thick Fe – 3% Si alloy in cold rolled condition. The total deformation was approximately 70%. The study of microstructure and texture was carried out with a scanning step of 0.1 and 0.025  $\mu\text{m}$  using the JEOL JSM6490LV raster electron microscope at an accelerating voltage of 20 kV. The estimated error limit of the crystal lattice orientation was on average  $\pm 0.6^\circ$ , but did not exceed  $\pm 1^\circ$ . Misorientations from 2 to  $15^\circ$  were marked as small angular boundaries between local volumes. High angles were detected when the misorientation was  $\geq 15^\circ$ .

A coordinate system was adopted with the following axes: cold rolling direction (RD), normal to its plane (ND), and the direction perpendicular to both (TD).

Using the matrix of rotation  $R$ , which was obtained from the ratio  $F_1 = RF_2$ , the misorientations between the crystal lattices of different orientations were determined. Where the matrix  $F$ , calculated from experimentally determined EBSD Euler angles, describes the orientation of the ferrite lattice. In the analysis to determine the closeness to the special misorientations of the CSL, the obtained matrices of rotation  $R$  were compared with the matrices corresponding to certain special misorientations from [25], by the method used in [26, 27]:

$$H_{ij} = C_j R^{-1} C_i T, \quad (1)$$

where matrix  $T_1$  is used as  $T$ , describing the variant of special misorientation of CSL from [25],

$C(C_j)$  – matrices of type  $\begin{pmatrix} 1 & 0 & 0 \\ 0 & 1 & 0 \\ 0 & 0 & 1 \end{pmatrix}$  describing in general 24 symmetrical turns in a cubic lattice:

$$i(j) = 1, 2, \dots, 24. \quad (2)$$

For each matrix of misorientation  $H$ , taking into account the full range of its symmetric variations, we calculated the values of angles  $\Theta$  and pivot axes  $[uvw]$ , using known mathematical formulas:

$$\Theta = \arccos\{[h_{11} + h_{22} + h_{33} - 1] / 2\}, \quad (3)$$

$$u : v : w = [h_{12} - h_{21}] : [h_{23} - h_{32}] : [h_{31} - h_{13}], \quad (4)$$

where  $h_{ij}$  are elements of  $H$  matrix. In the obtained sets of versions of deviation parameter values (angle and pivot axis) related to one  $H$  matrix, only one variant with the lowest angle value  $\Theta$  was chosen. Matrix  $T$  corresponding to the given version was accepted as the closest special misorientation of CSL, and corner  $\Theta$  was accepted as a deviation of experimentally defined orientation from orientation of CSL.

### 3. Results and discussion

The different propensity of different grain orientations to the formation of shear bands was established. Using orientation analysis of the microstructure with a large pitch (figure 1, a, b, c, grain I) it is shown that the banding does not occur in grains with an orientation close to  $\{001\}\langle 110\rangle$ .

Grains with orientation close to  $\{111\}\langle 112\rangle$  (figure 1, a, d, grain II) and  $\{111\}\langle 110\rangle$ ,  $\{112\}\langle 110\rangle$  (figure 1 a, b, c, grain III and IV) contain stripes. Only in some areas was it possible to determine the orientation within SBs. For example, in grain II, the orientation inside SB corresponds to  $\{110\}\langle 001\rangle$  (figure 1, d). This corresponds to the misorientation  $\Sigma 9$  (or  $\Sigma 27$ ) according to [21–23].

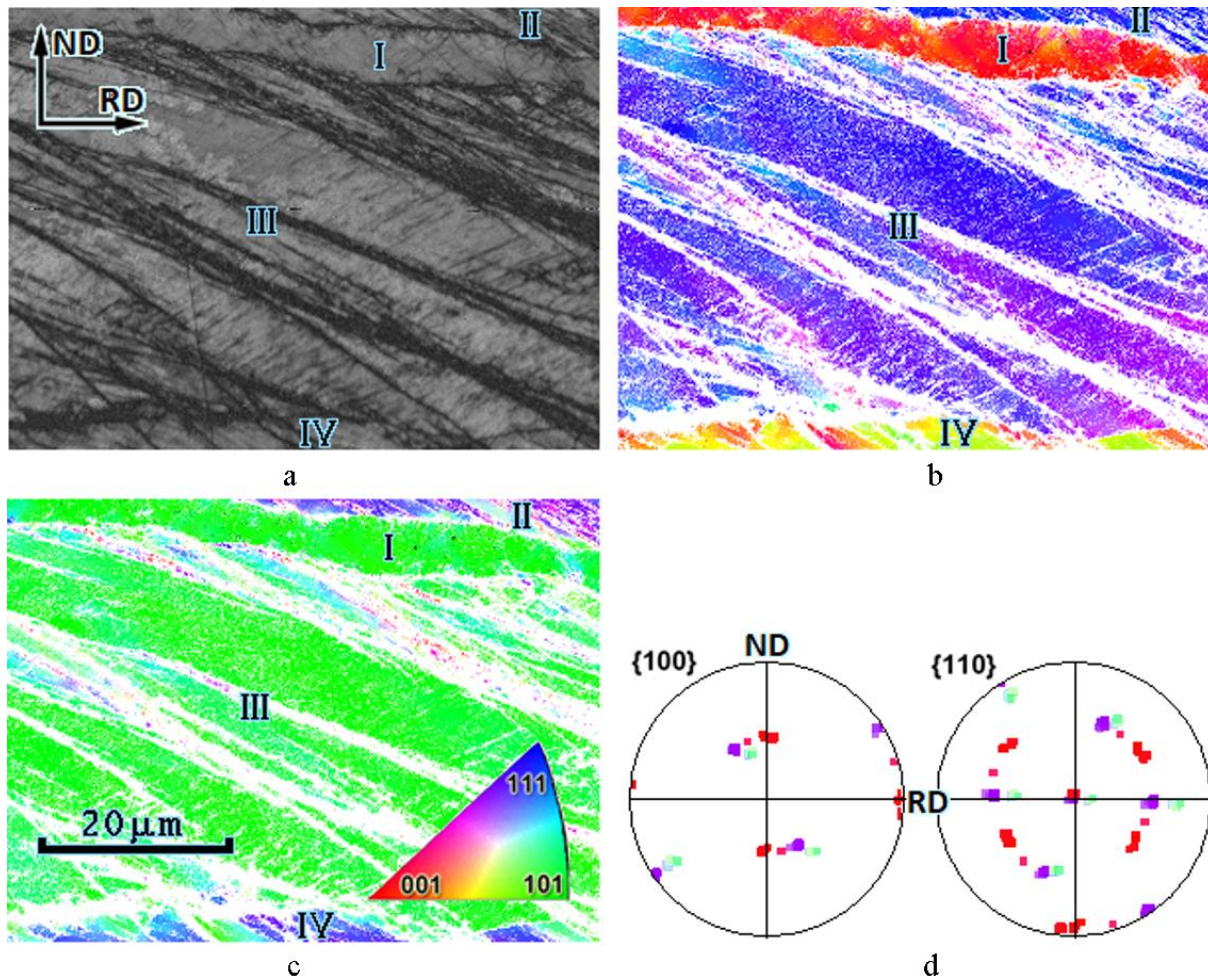


**Figure 1.** Microstructure of Fe-3%Si alloy polycrystal (4 grains: I, II, III, IV). Cold rolled state; deformation  $\varepsilon \sim 70\%$ ; EBSD: a – orientation map band contrast; b - orientation map from ND; c – orientation map from RD; d – DPF  $\{100\}$  and  $\{110\}$  of grain II.

The establishment of morphological and crystallographic features of SBs in grain with orientation close to  $\{111\}\langle 110\rangle$  (figure 2) was possible due to the increasing density of scanning points (step  $0.025 \mu\text{m}$ ). The fragment on figure 2 (a, b, c, d) contains three SBs characterized by close orientations in the central area, thus essentially differing in thickness (from  $0.5$  to  $1.5 \mu\text{m}$ ) and angles of a slope to a rolling plane  $\sim 20^\circ$ ,  $35^\circ$  and  $\sim 38^\circ$ . Presumably, SBs were formed at different points in time, i.e. at different values of deformation. The strips have a block structure. The blocks are stretched along the plane of habitus. The length of the blocks reaches  $2 \mu\text{m}$ . The number of blocks within the cross-section of wide SB varies from one to five. The misorientation between individual blocks can reach several tens of degrees. Central blocks of SBs have orientation close to  $\{110\}\langle 001\rangle$  with a significant magnitude of scattering (up to  $\sim 15^\circ$  around the axis  $\langle uv0\rangle$ ). On both sides of wide SBs the orientations of peripheral



blocks are close. The orientations of these blocks are related by rotation at angles of 15-25° around the  $\langle 110 \rangle$  axis close to the TD direction concerning the matrix orientation.

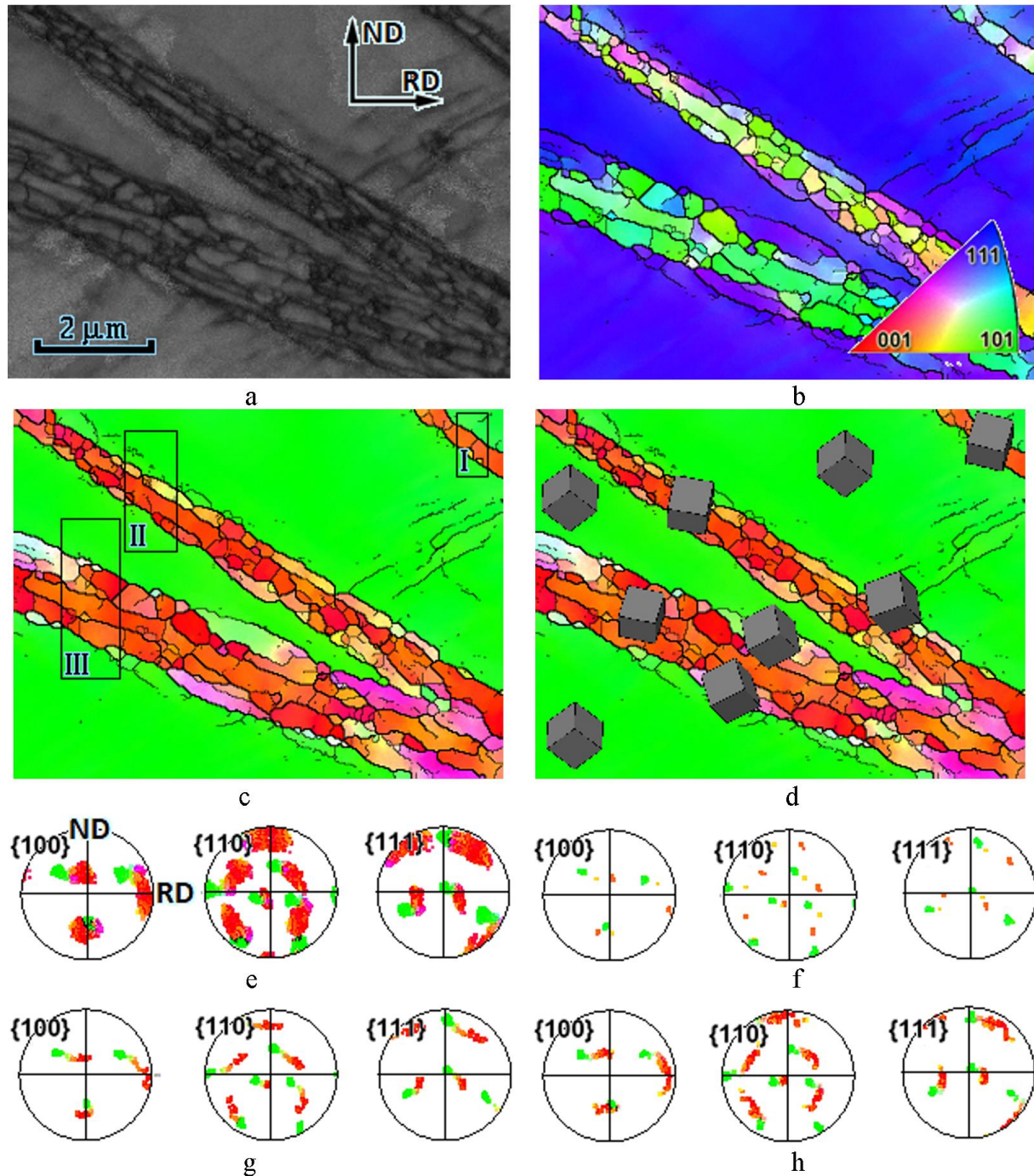


**Figure 2.** Microstructure and texture of Fe-3% Si single crystal  $\{111\}\langle 110 \rangle$ . Cold rolled state;  $\varepsilon \sim 70\%$ ; EBSD: a – orientation map band contrast; b – orientation map from ND; c – orientation map from RD; d – orientation map from RD, indicating orientations of individual structural elements in the form of elementary crystalline cells; e-h – DPF  $\{100\}$ ,  $\{110\}$ ,  $\{110\}$  corresponding to the micro areas marked with rectangles in “c”; e – areas shown in “c”; f – I; g – II; h – III.

The vector analysis allows us to describe the misorientation between the central units of all SBs and the matrix orientation  $\{111\}\langle 110 \rangle$  as CSL  $\Sigma 15 \pm (4-10^\circ)$  (rotation angle  $48.19^\circ$  around the axis  $\langle 210 \rangle$ ),

which does not coincide both with the misorientation of  $\Sigma 9$  (or  $\Sigma 27$ ) in deformed grains  $\{111\}\langle 112 \rangle$  and with the misorientation of  $\Sigma 5$  (or  $\Sigma 29a$ ) in deformed grains  $\{110\}\langle 110 \rangle$  [17], but in some sense is intermediate between them. It should also be noted that the correctness of the analysis is significantly affected by the orientation scattering, which continues due to the deformation of both the SBs and the matrix orientation and is reflected in the DPF (figure 2, e, f, g, h).

#### 4. Summary

Thus, it can be assumed that when the grain is banding with the orientation  $\{111\}\langle 110 \rangle$ , the matrix undergoes a sharp reorientation into the orientation  $\{110\}\langle 001 \rangle$  either due to the rotation around the  $\langle 100 \rangle$  axis (less likely) or due to the rotation around the  $\langle 110 \rangle$  axis (more likely). During further deformation, most of the SBs blocks are reoriented by dislocation sliding into orientations close to  $\{111\}\langle 112 \rangle$ , which play a significant role in subsequent recrystallization processes.

#### References

- [1] Lobanov M L, Redikultsev A A and Rusakov G M 2011 Electrotechnical anisotropic steel. Part I. history of development *Metal Science and Heat Treatment* **53** 326–332
- [2] Lobanov M L, Redikultsev A A and Rusakov G M 2011 Electrotechnical anisotropic steel. Part II. State-of-the-art *Metal Science and Heat Treatment* **53** 355–359
- [3] Ushioda K and Hutchinson W B 1989 *ISIJ Int.* **29** 862–867
- [4] Cruz-Gandarilla F, Penelle R and Mendoza-Leon H 2005 *Mater. Sci. Forum* **495–497** 483–488
- [5] Dorner D, Zaefferer S and Raabe D 2007 *Acta Mater.* **55** 2519–2530
- [6] Dorner D, Adachi Y, Tsuzaki K and Zaefferer S 2007 *Mater. Sci. Forum* **550** 485–490
- [7] SunMi Shin, SamKyu Chang and de Cooman B C 2008 *ISIJ Int.* **48** 1788–1794
- [8] Sokolov B K, Gubernatorov V V, Gervasyeva I V, Sbitnev A K and Vladimirov L R 1999 The Deformation and Shear Bands In The Fe-3%Si Alloy *Textures and Microstructures* **32** 21–39
- [9] Paul H, Driver J H, Maurice C and Jasien'ski Z 2003 Shear band microtexture formation in twinned face centred cubic single crystals *Materials Science and Engineering. A* **359** 178–191
- [10] Xue Q and Gray G T 2006 III Development of Adiabatic Shear Bands in Annealed 316L Stainless Steel: Part I. Correlation between Evolving Microstructure and Mechanical Behavior *Metallurgical and Materials Transactions A* **37A** 2436–2446
- [11] Dorner D, Zaefferer S and Raabe D 2007 Retention of the Goss orientation between microbands during cold rolling of an Fe3%Si single crystal *Acta Mater.* **55** 2519–2530
- [12] Dorner D, Adachi Y and Tsuzaki K 2007 Periodic crystal lattice rotation in microband groups in a bcc metal *Scripta Materialia* **57** 775–778
- [13] Peirs J, Tirry W and Amin-Ahmadi 2012 Microstructure of adiabatic shear bands in Ti6Al4V *Materials Characterization* **75** 79–92
- [14] Nguyen-Minh T, Sidor J J, Petrov R H and Kestens L A I 2012 Occurrence of shear bands in rotated Goss ( $\{110\}\langle 110 \rangle$ ) orientations of metals with bcc crystal structure *Scripta Materialia* **67** 935–938
- [15] Lobanov M L, Rusakov G M, Redikul'tsev A A, Karabanalov M S and Lobanova L V 2011 Shear Bands in Fe–3% Si–0.5% Cu Alloy *Steel in Translation* **41** 559–564
- [16] Rusakov G M, Lobanov M L and Redikul'tsev A A 2014 Lattice Reorientation in the Shear Bands of  $\{112\}\{131\}$  Crystallites in an Fe–3%Si Alloy *Technical Physics* **59** 1242–1244
- [17] Redikultsev A A, Rusakov G M and Lobanov M L 2018 The Possibility of Obtaining Electrical Steel with Texture  $\{100\}\langle 001 \rangle$  *Solid State Phenomena* **284** 483–488
- [18] Dillamore I L, Roberts J G and Bush A C 1979 Occurrence of shear bands in heavily rolled cubic metals *Mater. Sci.* **13** 73–77
- [19] Hutchinson J W and Tvergaard V 1981 Shear band formation in plane strain *International Journal of Solids and Structures* **17** 451–470
- [20] Mahesh S 2006 Deformation banding and shear banding in single crystals *Acta Materialia* **54** 4565–4574

- [21] Rusakov G M, Lobanov M L, Redikultsev A A and Kagan I V 2009 Model of  $\{110\}\langle 001 \rangle$  Texture Formation in Shear Bands during Cold Rolling of Fe-3 Pct Si Alloy *Metallurgical and materials transactions A* **40** 1023–1025
- [22] Rusakov G M, Redikul'tsev A A, Kagan I V and Lobanov M L 2010 Mechanism of Formation of Shear Bands upon Cold Deformation of a Commercial Fe-3% Si Alloy *The Physics of Metals and Metallography* **109** 662–669
- [23] Lobanov M L, Rusakov G M, Redikul'tsev A A and Lobanova L V 2013 Formation of Special Misorientations Related to Transition Bands in Structure of Deformed and Annealed Single Crystal (110)[001] of Fe-3% Si Alloy *The Physics of Metals and Metallography* **114** 27–32
- [24] Tailor G I 1938 Plastic strain in metals *Journ. Inst. Met.* **62** 307–324
- [25] Kaybyshev O A and Valiyev R Z 1987 *Grain boundaries and properties of metals* (Moscow: Metallurgiya) p 213
- [26] Kabanova I G and Sagaradze V V 1999 Statistical analysis of mutual misorientations of austenite (martensite) crystals after martensitic  $\gamma \rightarrow \alpha \rightarrow \gamma$  ( $\alpha \rightarrow \gamma \rightarrow \alpha$ ) transformations *The Physics of Metals and Metallography* **88** 44–52
- [27] Tereshchenko N A, Yakovleva I L, Kabanova I G and Mirzaev D A 2019 Special Misorientations in Low-Temperature Isothermal Bainite of High-Carbon Manganese–Silicon Steel *The Physics of Metals and Metallography* **120** 874–880

### Acknowledgments

The authors are grateful for assistance in the program of leading universities of the RF with the aim or improving their competitiveness No. 211 of the RF government No. 02.A03.21.0006.